Brain Tumor Pathol (2017) 34:120–129
DOI 10.1007/s10014-017-0291-y

ORIGINAL ARTICLE

Pericytes promote abnormal tumor angiogenesis in a rat RG2 glioma model

Junji Hosono[1,2] · Shunichi Morikawa[2] · Taichi Ezaki[2] · Takakazu Kawamata[1] · Yoshikazu Okada[1]

Received: 27 December 2016 / Accepted: 18 June 2017 / Published online: 23 June 2017

Abstract In glioma angiogenesis, tumor vessels cause morphological and functional abnormalities associated with malignancy and tumor progression. We hypothesized that certain structural changes or scantiness of functional pericytes may be involved in the formation of dysfunctional blood vessels in gliomas. In this study, we performed morphological examinations to elucidate the possible involvement of pericytes in brain tumor vessel abnormalities using a rat RG2 glioma model. After implantation of RG2 glioma cells in the syngeneic rat brain, gliomas were formed as early as day 7. In immunohistochemical examinations, desmin-positive pericytes, characterized by morphological abnormalities, were abundantly found on leaky vessels, as assessed by extravasation of lectin and high-molecular-weight dextrans. Interestingly, desmin-positive pericytes seemed to be characteristic of gliomas in rats. These pericytes were also found to express heat-shock protein 47, which plays an important role in the formation of the basement membrane, suggesting that RG2 pericytes promoted angiogenesis by producing basement membrane as a scaffold for newly forming blood vessels and caused functional abnormalities. We concluded that RG2 pericytes may be responsible for abnormal tumor angiogenesis lacking the functional ability to maintain the blood–brain barrier.

✉ Taichi Ezaki
ezakit@research.twmu.ac.jp

[1] Department of Neurosurgery, Tokyo Women's Medical University, 8-1, Kawada-cho Shinjuku-ku, Tokyo 162-8666, Japan

[2] Department of Anatomy and Developmental Biology, Tokyo Women's Medical University, 8-1, Kawada-cho Shinjuku-ku, Tokyo 162-8666, Japan

Keywords Glioma · Tumor angiogenesis · Pericyte · Blood–brain barrier · Rat

Introduction

Glioblastoma multiforme (GBM), the most common type of aggressive brain tumor in adults, exhibits high vascularization and relies on angiogenesis for tumor growth. Characteristic vascularized findings, such as microvascular proliferation appearing as "glomeruloid tufts", are pathological hallmarks of GBM [1]. These tumor microvascular networks are related to the supply of nutrients to growing tumors [2]. Various vascularization-promoting factors have been shown to be associated with the glioma microenvironment and to activate angiogenesis. The expression levels of vascular endothelial growth factor (VEGF), which is the most important factor promoting vascular angiogenesis, and its receptor (VEGF receptor [VEGFR]) are increased in high-grade gliomas (HGGs), particularly GBM [3]. Recently, the anti-VEGF monoclonal antibody bevacizumab was shown to be effective for the treatment of HGGs. However, the overall effects of bevacizumab on treatment outcomes are insufficient [4]. Thus, although anti-angiogenic treatment strategies have been investigated extensively, satisfactory curative effects have not been achieved. Therefore, additional studies are needed to further elucidate the mechanisms of angiogenesis to improve anti-angiogenic therapies.

The rat RG2 glioma model is a good representative model for typical human GBM, exhibiting a highly invasive and aggressive growth pattern [5, 6]. The histopathology of RG2 glioma in rats is classified as anaplastic or undifferentiated glioma [7], and previous reports have shown that RG2 gliomas are more aggressive

than C6 gliomas, as indicated by histological analyses [6, 7] and tumor-doubling time [6].

Recent studies have shown that tumor vessels have various structural abnormalities and dysfunctions [8]. In particular, the specialized structure and function of capillaries in the central nervous system (CNS) are critical [9–11]. Pericytes, forming the abluminal wall of brain capillaries, may promote angiogenesis [12, 13] and maintain the blood–brain barrier (BBB) [9]. Although many studies have focused on the glioma microenvironment, very few studies have evaluated the roles and morphological features of glioma vascular pericytes [8].

Therefore, we hypothesized that certain structural changes or scantiness of functional pericytes may be involved in the formation of dysfunctional blood vessels in gliomas. In this study, we investigated the process of angiogenesis and its sequential changes in an RG2 glioma model, with a primary focus on pericytes, which may play an important role in neurovascular formation and maintenance, using various morphological approaches.

Materials and methods

Rat glioma cell line

The rat glioma cell line RG2 was purchased from ATCC (CRL-2433; Manassas, VA, USA). RG2 cells were cultured in Dulbecco's modified Eagle's medium (DMEM; Life Technologies, Osaka, Japan) supplemented with 10% heat-inactivated fetal bovine serum (HyClone; Perbio Sciences), penicillin-G (10,000 U/mL; Sigma-Aldrich, St. Louis MO, USA), streptomycin (10,000 U/mL; Sigma-Aldrich), amphotericin-B (25 μg/mL), 2 mM L-glutamine (Life Technologies), 1 mM Na-pyruvate (Life Technologies), 10 mM HEPES (Life Technologies), and 50 μM 2-mercaptoethanol (Life Technologies). Cells were maintained in T-25 tissue culture flasks with 5% CO_2 in the air at 37 °C in a humidified incubator.

Animal model and microinjection of tumor cells

Four- or five-week-old female Fischer 344 rats weighing between 50 and 85 g were purchased from CLEA Japan, Inc. (Tokyo, Japan). Rats were maintained in air-filtered clean rooms and fed standard laboratory chow and water ad libitum. All animal care and experimental procedures throughout this study were performed according to the legislation of the Institute of Laboratory Animals for Animal Experimentation, Tokyo Women's Medical University (TWMU) and approved by the Animal Experiment Committee of TWMU. Unless otherwise stated, at least five rats per experimental group were examined. Under inhalation ether and intramuscular injection of 100 mg/kg ketamine and xylazine, a small burr hole was opened stereotactically 4 mm lateral from the bregma. RG2 cells (1×10^6 cells in 10 μL nutrient solution) were injected with a Hamilton 10-μL syringe into the right caudate nucleus (4 mm lateral from the bregma, 5 mm in depth), as previously reported [5, 14]. Ten microliters of the RG2 cell suspension was slowly injected over a 2-min period [5, 7, 15].

Tissue preparation

The mean survival time of rats after intracerebral implantation of RG2 cells was approximately 14 days. According to a previous report [16], we defined days 7, 10, and 14 after the cell implantation as early, intermediate, and advanced stages, respectively. Sample tissues from each stage and normal tissues from 5-week-old rats as controls were examined. All animals were killed by cardiac perfusion with 4% paraformaldehyde (PFA) in phosphate-buffered saline (PBS; pH 7.2) through the ascending aorta at a pressure of 120 mmHg for 10 min. Brain tissues were subsequently excised, infiltrated overnight with 30% sucrose, and frozen with optimum cutting temperature (OCT) cryostat-embedding compound (Tissue-Tek, Torrance, CA, USA) by snap freezing in liquid nitrogen. Cryosections (at 12 or 120 μm thickness) were made with a cryostat (Leica, CM1850, Leica Microsystems K.K., Takadanobaba, Tokyo, Japan). For semi-thin section observation, immediately after cardiac perfusion, brain tissues were cut into small pieces and immersed in 4% PFA and 2.5% glutaraldehyde in PBS for another 2 h. Specimens were then treated with 1% osmium tetroxide for 2 h at 4 °C and with uranyl acetate for 3 h at room temperature (typically 20–24 °C). Thereafter, the specimens were dehydrated in a graded series of ethanol and finally embedded in epoxy resin. Semi-thin sections (0.5 μm in thickness) were made and stained with toluidine blue for light microscopy.

Labeling of blood vessels with tomato lectin

Fluorescein isothiocyanate (FITC)-labeled tomato lectin (*Lycopersicon esculentum* lectin; Vector Laboratories, Burlingame, CA, USA; 300 μg in 150 μL of 0.9% NaCl) was injected into the femoral vein and allowed to circulate for 10 min before perfusion of fixative [17].

Evaluation of vascular leakage with Evans blue and FITC dextrans

To evaluate vascular leakage, 1% Evans blue (Wako, Osaka, Japan) in 300 μL of 0.9% NaCl was intravenously

(i.v.) injected to circulate for 30 min before perfusion fixation, and three FITC-dextrans (Sigma-Aldrich) of different molecular sizes (molecular weights: 25, 50, and 200 kDa) were also used. FITC-dextrans (0.5 mL of a 100 mg/mL solution in 0.9% NaCl) were administered i.v. to circulate for 2 min before perfusion fixation. Cryosections were prepared at a thickness of 12 μm. Specimens were rinsed several times with PBS (pH 7.4) to dissolve the OCT compound. Sections were then directly mounted on cover slips using Vectashield (Vector Laboratories) [18] and examined with a Keyence BZ9000 All-in-One microscope (Keyence Co. Higashi-Nakajima, Osaka, Japan).

Immunohistochemistry

The following antibodies for immunofluorescence were used. A mouse monoclonal antibody against rat endothelial cell antigen (RECA-1; 1:100, mouse; Abcam, Inc., Cambridge, UK) was used for endothelial cell (EC) identification, an anti-laminin antibody (1:500, chicken polyclonal; Abcam) was used for identification of the basement membrane, and anti-desmin (1:2000, rabbit polyclonal; Abcam; or 1:100, rabbit monoclonal; Cell Signaling Technology, Tokyo, Japan) and anti-platelet-derived growth factor receptor beta (PDGFRβ; rabbit monoclonal; Thermo Fisher Scientific Inc., Waltham, MA, USA) antibodies were used for pericyte identification. Antibodies were diluted in PBS containing 1% bovine serum albumin (BSA) for application on 12-μm sections or 0.5% Triton-X plus 1% BSA in 1× PBS for application on 120-μm sections. Using the injected tomato lectin model, RECA-1 was detected with donkey anti-mouse immunoglobulin (Ig) secondary antibodies labeled with Cy3 (Jackson ImmunoResearch, West Grove, PA, USA) to examine structural changes in the vascular network. Pericytes were assessed by double immunostaining for desmin or PDGFRβ and RECA-1, and secondary donkey anti-rabbit Ig antibody labeled with Alexa Fluor 647 (Jackson ImmunoResearch) and a donkey anti-mouse Ig labeled with Cy3, respectively, were used for detection. For staining, sections measuring 120 μm thick were incubated at room temperature for 48 h in a mixture of each of the primary antibodies described above. After several washes with 0.5% Triton X in 1× PBS, specimens were incubated overnight at room temperature with a mixture of each secondary antibody. Subsequently, specimens were fixed with 4% PFA, washed several times with PB, and mounted using Vectashield. In the same way, triple immunofluorescence staining using laminin, RECA-1, and desmin was performed to examine the structure of the vascular basement membrane. The following secondary antibodies were used: donkey anti-chicken Ig antibodies labeled with Alexa Fluor 647 for laminin staining, donkey anti-mouse Ig antibodies labeled with FITC for RECA-1 staining, and donkey anti-rabbit Ig antibodies labeled with Cy3 for desmin staining, respectively (all antibodies were from Jackson ImmunoResearch). To evaluate pericyte function, triple immunostaining was performed with anti-desmin antibodies, anti-laminin antibodies, and mouse monoclonal antibodies to heat-shock protein 47 (HSP47; LSBio), a collagen-binding protein. Sections measuring 12 μm thick were incubated at room temperature overnight in a mixture of all antibodies. After several washes with PBS, specimens were incubated for 3 h at room temperature with the following secondary antibodies: donkey anti-rabbit Ig antibody labeled with FITC for desmin staining, donkey anti-mouse Ig antibody labeled with Cy3 for HSP47 staining, and donkey anti-chicken Ig antibody labeled with Alexa Fluor 647 for laminin staining (all antibodies were from Jackson ImmunoResearch). All stained samples were examined with a Leica TCS-SL confocal laser-scanning microscope (Leica, Wetzlar, Germany).

Real-time quantitative reverse transcription polymerase chain reaction (qRT-PCR)

Total RNA was extracted from PBS-injected brains (control) and RG2 tumor brains (day 14) using Isogen (Nippon Gene, Toyama, Japan). cDNA was synthesized using SuperScript III reverse transcriptase (Invitrogen, Carlsbad, CA, USA) [19]. For expression analyses, *desmin* (Genbank: NM_022531.1) and *PDGFRβ* (Genbank: NM_031525.1) were amplified using the following primers: *desmin* sense, 5′-AGGGACATCCGTGCTCAGTA-3′; *desmin* antisense, 5′-AGCATCAATCTCGCAGGTGT-3′; *PDGFRβ* sense, 5′-TGTTCGTGCTATTGCTCCTG-3′; *PDGFRβ* antisense, 5′-TGTCAGCACACTGGAGAAGG-3′; TATA box-binding protein (TBP) sense, 5′-GCGGGGTCATGAAATCCAGT-3′; TBP antisense, 5′-CGTCACGCACCATGAAACAG-3′ [20].

Evaluation of the proliferation of vascular endothelial cells and pericytes

Quantitative analyses of pericytes and vascular ECs were performed using five samples on days 7, 10, and 14 ($n = 5$). The ratios of positive areas for either RECA-1 or desmin in the whole visual area were estimated as endothelial proliferation and pericytes, respectively, with the ImageJ software (NIH, USA).

Statistical analysis

Differences with P values of less than 0.05 were considered statistically significant according to two-sample t tests.

Results

Development of tumor blood vessels during RG2 glioma progression

After cell transplantation, RG2 gliomas formed huge tumor masses in the cerebral hemisphere by day 14 (Fig. 1a, b). Blood vessels in RG2 gliomas (Fig. 1d, f) showed irregular sizes and morphologies in comparison with those of normal brain vessels (Fig. 1c, e). The structural abnormalities of vessels, such as tortuousness, dilation, and glomeruloid changes, became more dramatic during tumor development (Fig. 2a–c). The glioma vascular network developed over time with tumor progression (Fig. 2d–i). Vascular development was accelerated from day 10 after tumor inoculation. In addition to the increased morphological abnormalities over time (Fig. 2a–c), the blood flow within the gliomas also became heterogeneous during tumor progression (Fig. 2d–i). Because tomato lectin is a glycoprotein that binds the sugar chain of the endothelial luminal surface and can be used to detect the presence of blood flow, we found that the number of dysfunctional vessels without blood flow increased over time after application of tomato lectin i.v. on days 7, 10, and 14 after glioma inoculation (Fig. 2d–i).

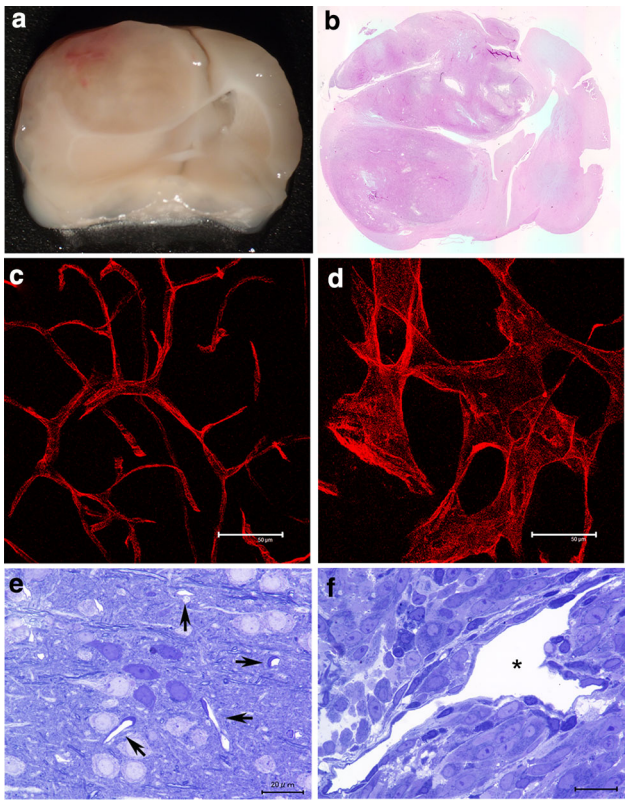

Fig. 1 Macroscopic views of RG2 glioma and microscopic comparisons of blood vessels with normal control brain tissues. Macroscopic appearance (**a**) and a coronal cryosection stained with hematoxylin and eosin (**b**) on day 14 after RG2 glioma implantation. (**c–f**) Morphological comparison between normal brain microvessels (**c**, **e**) and RG2 glioma vessels (**d**, **f**). Confocal microscopic images of RECA-1 immunoreactivity of ECs (**c**, **d**) and semi-thin sections (**e**, **f**). Normal vessels with uniform vessel diameters and sizes were distributed regularly (arrows in **e**). In contrast, tumor vessels showed various sizes and irregular shapes. *Asterisk* Vascular lumens (**f**). *Scale bars* 50 μm (**c**, **d**), 20 μm (**e**, **f**). Day 14 RG2 models were generated using 20 rats (a), and representative sample sections (b–f) were stained using five individual rats ($n = 5$)

Characteristics of blood vessels in RG2 glioma

Multiple-immunostaining revealed that glioma vessels were completely covered by the vascular basement membrane during the whole time course of tumor development similar to normal vessels, as observed on day 7 (Fig. 3a, b). However, regarding pericytes, glioma vessels also exhibited several features that were not observed in normal brain vessels (Fig. 3c, d, f, g). When compared with normal pericytes, glioma pericytes had multiple cytoplasmic processes and tended to project these processes into the perivascular space (Fig. 3g). Many of these processes bridged vessels that were separate from each other (Fig. 3g). Moreover, although normal brain pericytes usually express PDGFRβ but not desmin (Fig. 3c, f) in rats, glioma pericytes expressed both markers (Fig. 3d, g). Desmin expression was examined using two different antibodies from separate commercial companies to increase the reliability of the results; similar findings were observed using both antibodies. In contrast, PDGFRβ immunoreactivity tended to be stronger in RG2 pericytes than in normal controls (Fig. 3c, d). To evaluate the reactivity of immunostaining objectively, qRT-PCR was performed to assess *desmin* and *PDGFRβ* expression (Fig. 3e, h). The expression levels of both genes significantly increased compared with those of the control. In particular, the expression of *desmin* increased significantly in the tumor environment.

Abnormal permeability in glioma vessels

As a functional study, we used two different particles to investigate vascular permeability during glioma progression. Extravasation of Evans blue was observed throughout the entire tumor on day 14 as early as 30 min after injection (Fig. 4a). To assess the vascular permeability of glioma vessels in detail, we used dextrans of different molecular sizes (25, 50, and 200 kDa) on days 7, 10, and 14. Permeability was dramatically elevated from day 10 after glioma inoculation, and dextrans as large as 200 kDa were extravasated from vessel walls (Fig. 4b–d). When lectin-perfused specimens were closely observed with a

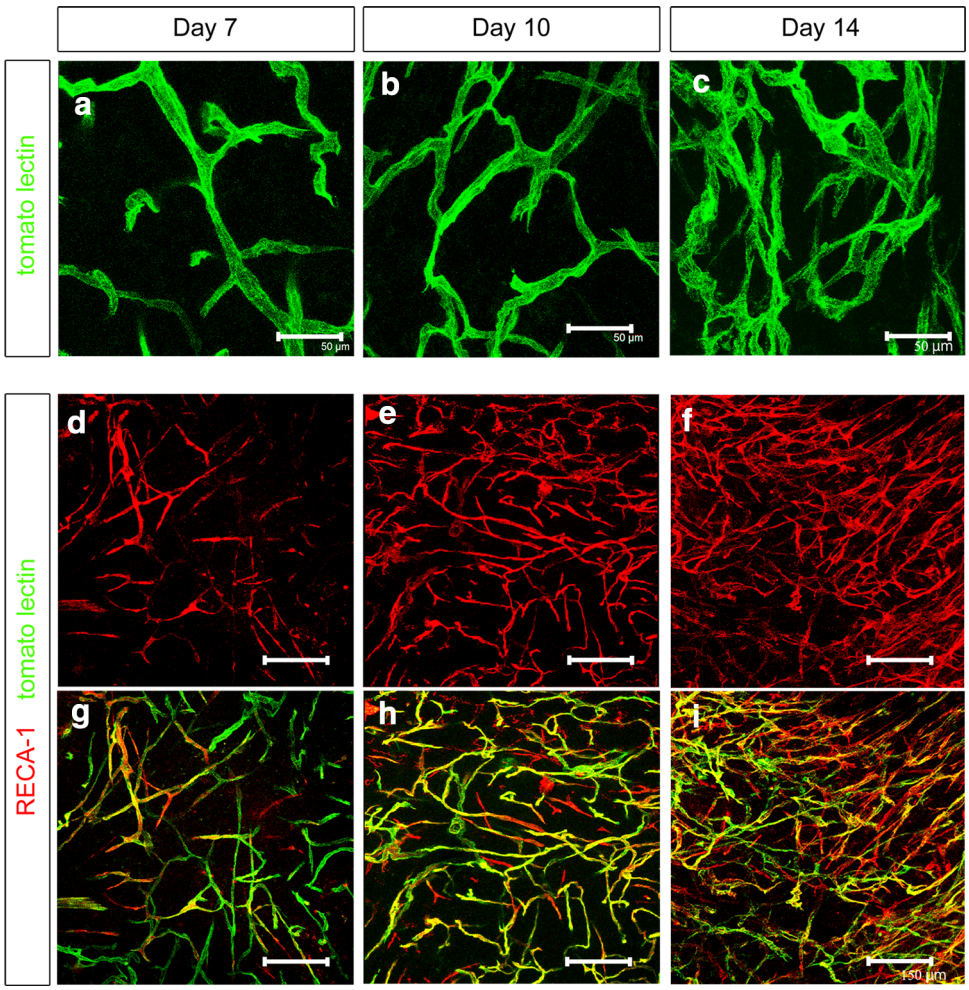

Fig. 2 Changes in the morphology and density of blood vessels during RG2 progression. Confocal microscopic images of double-staining for tomato lectin, shown in green (**a–c**, **g–i**), and RECA-1, shown in red (**d–i**). Observation at the early stage (day 7: **a**, **d**, **g**), intermediate stage (day 10: **b**, **e**, **h**), and advanced stage (day 14: **c**, **f**, **i**). Morphological abnormalities in tumor vessels. Angioarchitecture similar to normal vessels at the early stage (**a**). Tortuous and dilated vessels were increased during the intermediate stage (**b**). Microvascular proliferations, such as "glomeruloid tufts," in the advanced stage (**c**). **d–i** Changes in the glioma microvascular network over time. The tumor vascular network showed a tendency to develop over time, increasing dramatically after day 10. In addition, the blood distribution in the tumor also became heterogeneous over time, and dysfunctional vessels without blood flow (RECA-1 positive and lectin negative) increased in connection with tumor expansion. *Scale bars* 50 µm (**a–c**), 150 µm (**d–i**). The fluorescent image shows a representative sample section from five individual rats ($n = 5$)

higher magnification, extravasated lectin was observed around vessel walls (Fig. 4e).

Quantitative analyses of vascular endothelial cells and pericytes in RG2 gliomas

A quantitative analysis showed that in glioma vessels, the numbers of vascular ECs did not increase from day 7 to day 10, whereas the number of pericytes more than doubled (Fig. 5a). In addition, the number of ECs increased rapidly from day 10 to day 14, indicating that the increase in pericytes preceded the increase in ECs. Interestingly, the number of pericytes continued to increase during tumor progression (Fig. 5b–d).

Bridging of newly formed tumor vessels by pericytes and expression of markers of basement membrane production in RG2 gliomas

At the early stage of tumor progression (day 7), there were many sites where blood vessels were bridged by sprouting pericytes. Interestingly, when these sites were closely analyzed, we found that the vascular basement membrane had already been formed between these vessels without any

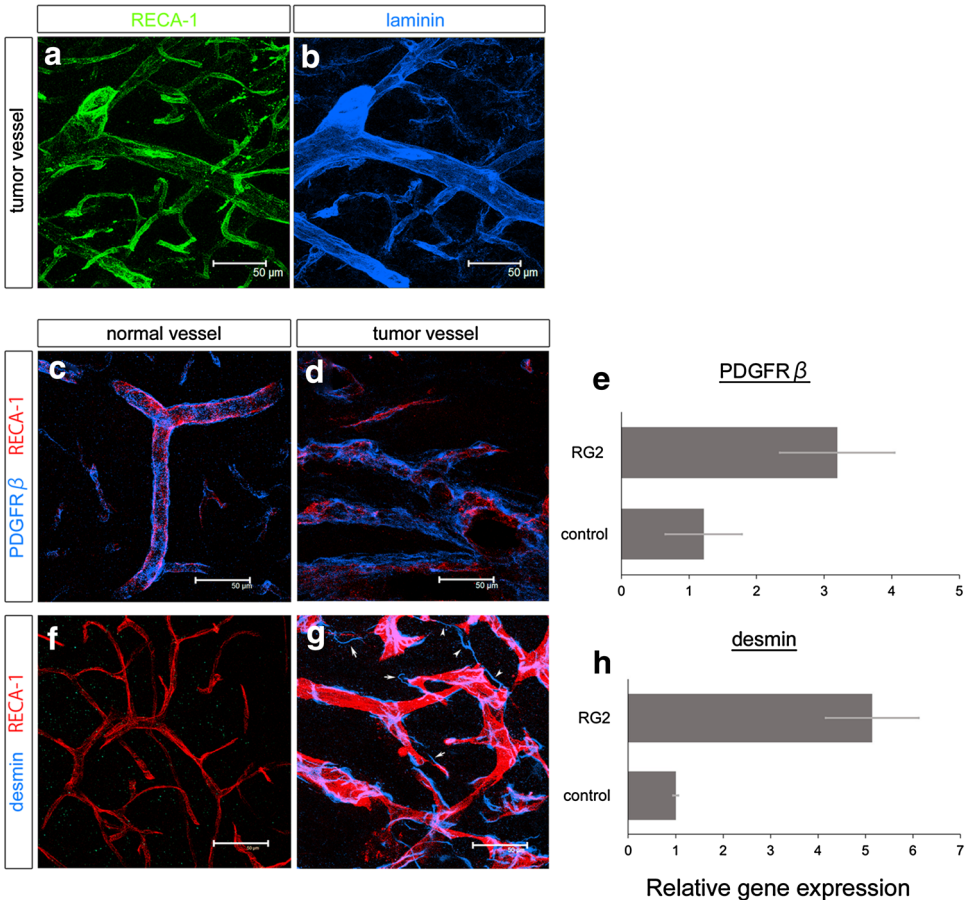

Fig. 3 Characterization of the basement membrane and pericytes in RG2 glioma vessels using specific markers. The basement membrane was examined by double immunostaining for RECA-1 (ECs) and laminin (basement membrane). Confocal microscopic images of RECA-1 immunoreactivity in ECs (*green* **a**) and laminin immunoreactivity of basement membranes (*blue* **b**). **a**, **b** Vascular walls of tumor vessels in the early development stage (day 7). Mature vascular walls are constructed from the early stage. Tumor pericytes are identified by two different pericyte markers (day 14): PDGFRβ (*blue* **c**, **d**) and desmin (*blue* **f**, **g**) in combination with RECA-1 (*red*). PDGFRβ (**c**, **d**) or desmin (**f**, **g**) immunoreactivities of pericytes are shown in blue. PDGFRβ-positive pericytes were expressed around the surfaces of the vessels (**c**, **d**). In particular, pericytes on tumor vessels tend to be expressed more strongly than that on normal vessels. Note that desmin-positive pericytes were expressed around tumor vessels but not around normal vessels (**f**, **g**). Glioma pericytes had abnormal structures, such as multiple cytoplasmic processes, protrusion toward the stroma (*arrows* in **g**), and bridging between these processes (*arrowheads* in **g**). *Scale bar* 50 μm. The fluorescent image shows a representative sample section from five individual rats ($n = 5$). Relative expression of *PDGFRβ* and *desmin* genes in RG2 tumor and control groups was determined by qRT-PCR analyses (**e**, **h**)

ECs (Fig. 6a–c). To examine whether these desmin-positive pericytes had the ability to produce basement membrane, HSP47, a molecular chaperone that is necessary for type IV collagen production, was evaluated by immunostaining. As a result, we found that HSP47 expression was colocalized in desmin-expressing pericytes (Fig. 6d–f).

Discussion

In the present study, we characterized the abnormal blood vessels that formed in a rat glioma model using immunohistological analyses and found that pericytes may be responsible for both morphological and functional abnormalities of tumor vessels. We observed extensive angiogenesis along with RG2 glioma growth after transplantation into normal syngeneic rats. This high angiogenic potential was deeply related to its aggressive growth. During angiogenesis, the vascular network within the RG2 gliomas showed increasing disorganization, including irregular diameters and abnormal branching patterns. Furthermore, the vessels did not fit into the usual categorization of arterioles, capillaries, or venules and often formed collapsing huge sinus-like spaces in the tumor. In addition, there were fewer functional vessels with blood flow within the network, and increased numbers of vessels with higher vascular permeability were observed.

In this study, we examined the possible mechanisms involved in the abnormal angiogenesis in RG2 glioma, with a focus on the basement membrane and pericytes, which,

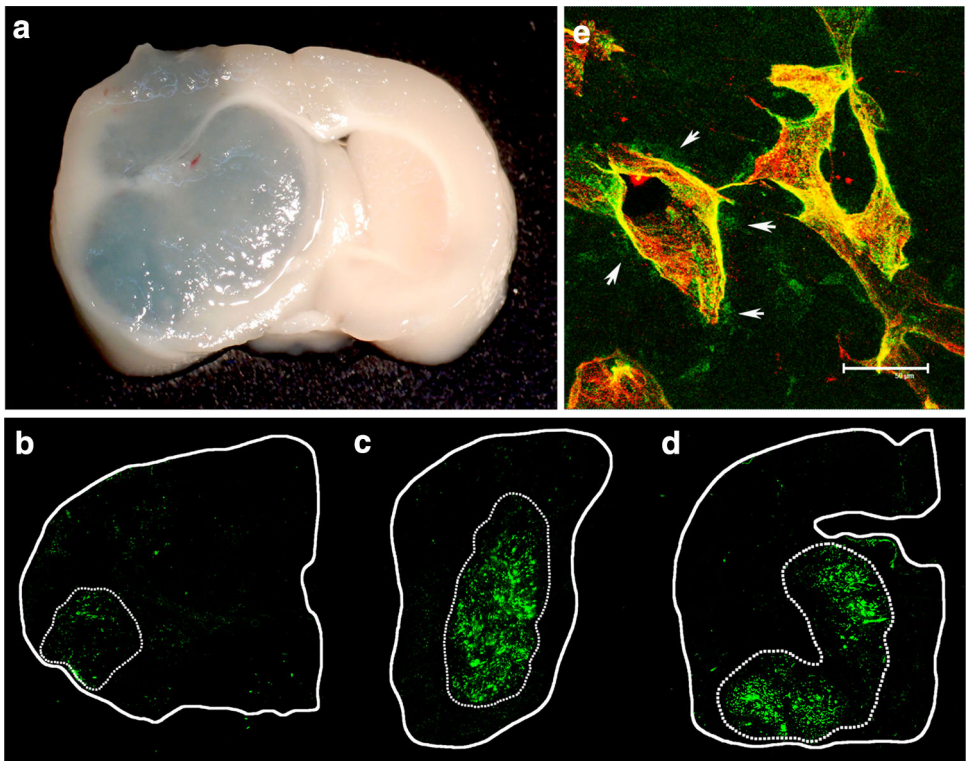

Fig. 4 Functional studies of the BBB, as assessed by the vascular leakage of differently sized molecules. **a** Macroscopic appearance after intravenous injection of Evans blue. Intratumoral tissues were colored in blue due to extravasation from tumor vessels. Injection of high-molecular-weight (200 kDa) FITC dextran. Samples from days 7 (**b**), 10 (**c**), and 14 (**d**) are shown. *Dotted lines* indicate the boundaries of RG2 gliomas (**b-d**). High-molecular-weight dextran leaked through the vascular wall from the early stage (**b**). The leakage became more dramatic as the tumor vascular network developed. (**e**) Fluorescence micrograph showing tumor vessels in RG2 gliomas double-stained for RECA-1 (*red*) and tomato lectin (*green*). Leakage of tomato lectin was observed in the abluminal endothelial wall (*arrows*). *Scale bar* 50 μm. The fluorescent image shows a representative sample section from five individual rats ($n = 5$)

along with ECs, are components of the BBB. Various differences have been reported between normal and glioma ECs [21]; however, our study revealed several differences in pericytes as well. Similar to blood vessels in the normal CNS, RG2 glioma vessels contained pericytes entirely covered with the basement membrane, which appeared to be morphologically normal. However, RG2 pericytes were different from normal CNS pericytes based on various parameters.

The most remarkable features of RG2 pericytes are their possible angiogenic potential. First, we found that RG2 pericytes increased in number just before the major increase in the number of ECs. These pericytes were associated with proliferating ECs, projected multiple cytoplasmic processes into stromal space, and bridged blood vessels that were separated. These features suggest that pericytes may have a guiding role in the angiogenic process. Pericytes are often described in the context of a stabilizer of the vessel wall [9]. However, promotion of angiogenesis by pericytes has also been suggested in various angiogenic processes, such as the ovarian cycle, normal growth of mesentery vessels, wound healing, chemically induced inflammation, and tumors [17, 22–26]. Previously, we have reported that in dermal wound healing, pericyte precursors are recruited to the wounded site to induce angiogenesis and are later incorporated into the newly formed vessel wall [26].

Second, in the case of RG2 pericytes, we should pay special attention to the possible role in basement membrane production as a scaffold for newly forming vessels by ECs, because we found that RG2 pericytes expressed HSP47, which is not generally expressed in normal CNS pericytes [27]. HSP47, a type IV collagen-specific molecular chaperone, plays an important role in the formation of the basement membrane [28, 29]; thus, the presence of this protein implied that these pericytes had the ability to produce basement membrane. In addition to type IV collagen, in vivo studies have revealed their potential to produce multiple isoforms of laminin, which is also a crucial component of the basement membrane [30]. Similar to the present study of RG2 gliomas, guidance for newly forming vascular endothelial sprouts by pericytes through basement membrane production has also been suggested in mammary tumor models [25]. Moreover, HSP47 is also thought to promote tumor angiogenesis by activating hypoxia-inducible factor (HIF)-1α via the VEGF signaling pathway

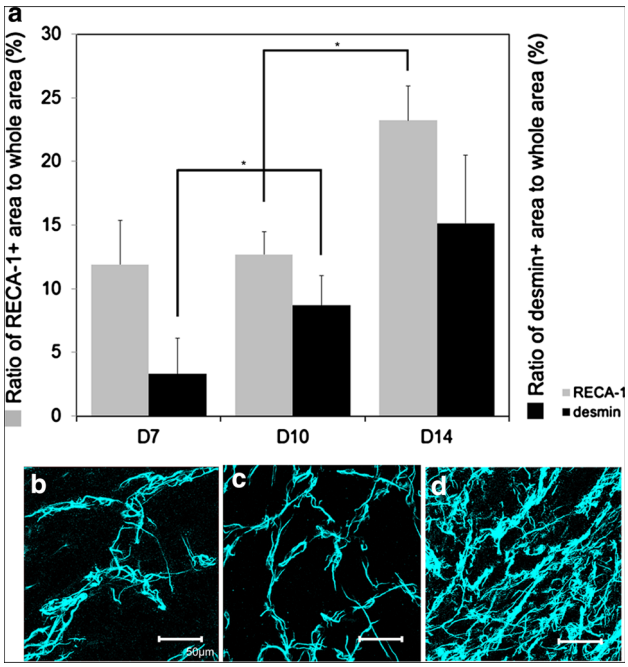

Fig. 5 Quantitative analyses of vascular endothelial cells and pericytes. **a** Proliferation of vascular pericytes or ECs in RG2 gliomas was evaluated by determining the ratios of desmin- or RECA-1-positive areas to the total area in the high-power field (×63). Increased numbers of pericytes were observed, followed by EC proliferation. Fluorescence micrographs of desmin immunoreactivity of pericytes (*blue*). Samples from day 7 (**b**), day 10 (**c**), and day 14 (**d**) are shown. Pericytes increased constantly and dramatically over time. Five samples were analyzed for each group ($n = 5$). *$P < 0.05$ for comparisons between two groups

[28]. Taken together, these data suggested that HSP47-expressing RG2 pericytes may promote angiogenesis.

However, it is still possible that basement membrane lacking endothelium does not indicate the angiogenic process, but rather represents a site of vessel regression [31, 32]. Both the formation and regression of blood vessels can generally occur during the course of tumor progression [33]; thus, we cannot exclude the possibility that these observations were indicative of the vascular regression process. However, some recent studies of tumors have suggested that vascular regression is usually accompanied by the detachment of pericytes and smooth muscle cells [33, 34]. Furthermore, other studies have reported that the existence of pericytes is necessary for endothelial survival [35, 36]. Therefore, although it is still possible that our findings represent vessel regression, we believe that these studies support our hypothesis that vascular basement membrane structures lacking ECs, but still, harboring pericytes may represent sites of vascular remodeling. In addition, the observation that many regressing blood vessels found in tumors were exclusively composed of vascular basement membranes and lacked both ECs and pericytes may also support our hypothesis [31].

RG2 pericytes are different from normal CNS pericytes in several other aspects. For example, normal CNS pericytes closely interact with ECs through various signaling pathway to form and maintain the BBB [9, 10, 35]. Although BBB dysfunction is often found in various brain diseases, in the case of gliomas, it is unclear whether altering pericyte properties may cause BBB dysfunction. Because RG2 vessels show increased permeability during angiogenesis, RG2 pericytes may not have the capacity to tightly control permselectivity. In addition to differential expression of HSP47, RG2 pericytes also exhibited variations in marker expression compared with normal CNS pericytes. Normal CNS pericytes in rats typically expressed PDGFRβ but not desmin, whereas RG2 pericytes expressed both PDGFRβ and desmin. The PDGF signaling pathway is known to recruit pericytes to sites of new vessel formation [13, 36, 37]. Thus, our findings that PDGFRβ immunoreactivity and related gene expression were stronger in RG2 pericytes than in normal pericytes may suggest the active recruitment of pericyte precursors for angiogenesis. In contrast, desmin is an intermediate filament of myoid cells [23, 36, 38, 39], and in the case of rats, all pericytes found in the entire body other than CNS (except for vascular smooth muscle cells of arterioles or venules) express this critical protein. In this study, we reported, for the first time, that desmin was expressed in pericytes in rat brain tumors. Analyses of *desmin* and *PDGFRβ* via qRT-PCR suggested that angiogenesis (with increasing numbers of desmin-positive pericytes) was activated under the RG2 tumor environment. An increase in desmin-positive pericytes preceded basement membrane and vascular endothelial formation. Thus, RG2 pericytes exhibited various differences compared with their normal counterparts in terms of morphology and functional roles. These abnormal pericytes may participate in promoting tumor angiogenesis and tumor progression.

Conclusion

The present study revealed various abnormal features of pericytes, including morphology, marker expression, and possible functional roles, in RG2 glioma. Additional detailed studies on marker expression are needed to further characterize the physiological features and origins of RG2 pericytes. These abnormal pericytes appeared to promote angiogenesis and affect tumor growth. The characteristics of abnormal pericytes are specialized and may be responsible for vascular formation, resulting in rapid tumor progression. Alternatively, these pericytes, as a neurovascular unit of the BBB, may lose their abilities to mediate vascular stabilization and maintain vascular homeostasis. Therefore, targeting the suppression of abnormal pericyte development may lead

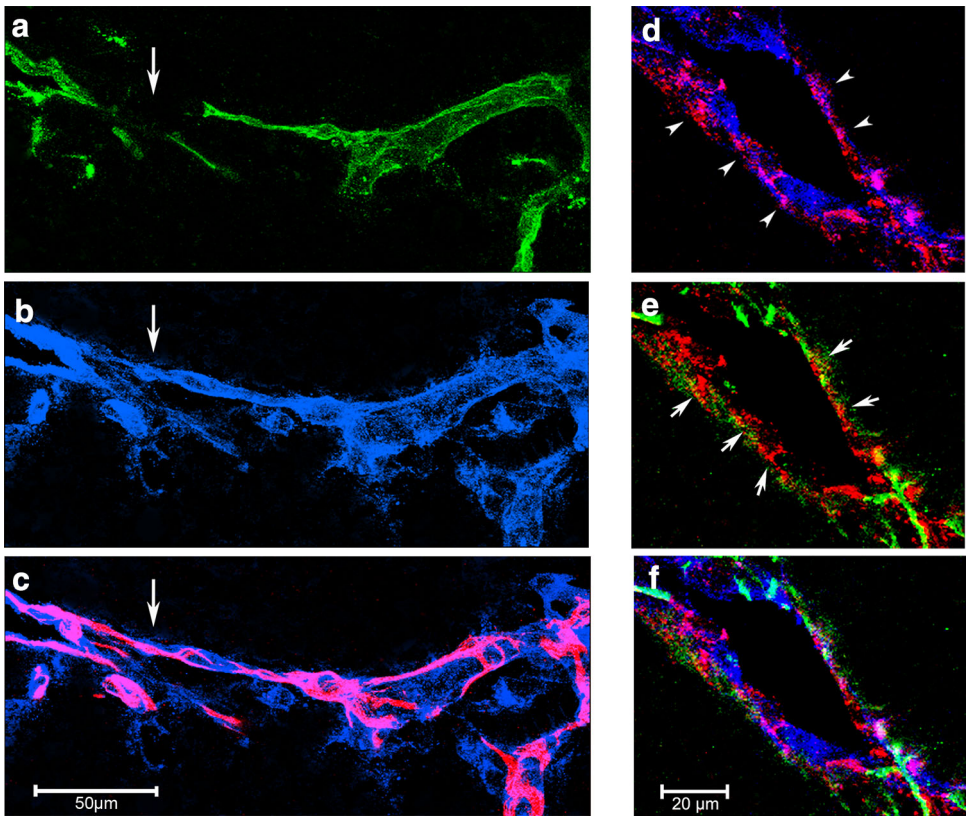

Fig. 6 Role of pericytes in newly forming vessels in RG2 gliomas. Confocal microscopic images of multiple-immunofluorescence staining in an RG2 glioma during the early stage (day 7). Cryosections of 120-μm thickness (**a–c**) were made and stained for RECA-1 (EC marker; *green*; **a**), laminin (basement membrane marker; *blue* **b**, **c**), and desmin (pericyte marker; *red* **c**). Immature vessel walls consisted of basement membranes without ECs (*arrows* in **a**, **b**). At this site, tumor vessels were bridged by sprouting of pericytes (*arrow* in **c**). Cryosections of 12-μm thickness were stained for laminin (*blue*), HSP47 (*red*), and desmin (*green*). **d** Combination of laminin (*blue*) and HSP47 (*red*). **e** A combination of desmin (*green*) and HSP47. **f** Merged view. The distribution of HSP47 was similar to that of laminin (*arrowheads* in **d**). Furthermore, there were many sites at which the expression levels of HSP47 and desmin were overlapped in tumor vessels (*arrows* in **e**), demonstrating that pericytes had the ability to produce basement membranes. *Scale bar* 50 μm (**a–c**), 20 μm (**d–f**). The *fluorescent image* shows a representative sample section from five individual rats ($n = 5$)

to prevention of tumor angiogenesis and progression. Our findings may provide insights into effective treatment strategies by targeting tumor angiogenesis in HGGs.

Acknowledgements The authors would like to thank Ms. Aya Matsui and Ms. Kazuko Nakada (Department of Anatomy and Developmental Biology, Tokyo Women's Medical University) for their excellent technical support and Ms. Matsui in particular for assistance with the qRT-PCR analyses. The authors would also like to thank Dr. Yoshihiro Muragaki and Dr. Masayuki Nitta (Department of Neurosurgery, Tokyo Women's Medical University) for valuable advice and critical reviews of the manuscript.

Compliance with ethical standards

Conflict of interest The authors declare that they have no conflicts of interest.

References

1. Hardee ME, Zagzag D (2012) Mechanisms of glioma-associated neovascularization. Am J Pathol 181:1126–1141
2. Wesseling P, Ruiter DJ, Burger PC (1997) Angiogenesis in brain tumors; pathobiological and clinical aspects. J Neurooncol 32:253–265
3. Plate KH, Breier G, Weich HA et al (1992) Vascular endothelial growth factor is a potential tumour angiogenesis factor in human gliomas in vivo. Nature 359:845–848
4. Gilbert MR, Dignam JJ, Armstrong TS et al (2014) A randomized trial of bevacizumab for newly diagnosed glioblastoma. N Engl J Med 370:699–708
5. Aas AT, Brun A, Blennow C et al (1995) The RG2 rat glioma model. J Neurooncol 23:175–183
6. He T, Smith N, Saunders D et al (2013) Molecular MRI differentiation of VEGF receptor-2 levels in C6 and RG2 glioma models. Am J Nucl Med Mol Imaging 3:300–311
7. Barth RF, Kaur B (2009) Rat brain tumor models in experimental neuro-oncology: the C6, 9L, T9, RG2, F98, BT4C, RT-2 and CNS-1 gliomas. J Neurooncol 94:299–312
8. Jain RK, di Tomaso E, Duda DG et al (2007) Angiogenesis in brain tumours. Nat Rev Neurosci 8:610–622
9. Winkler EA, Bell RD, Zlokovic BV (2011) Central nervous system pericytes in health and disease. Nat Neurosci 14:1398–1405
10. Vallon M, Chang J, Zhang H et al (2014) Developmental and pathological angiogenesis in the central nervous system. Cell Mol Life Sci 71:3489–3506

11. Daneman R, Zhou L, Kebede AA et al (2010) Pericytes are required for blood-brain barrier integrity during embryogenesis. Nature 468:562–566
12. Ribatti D, Nico B, Crivellato E (2011) The role of pericytes in angiogenesis. Int J Dev Biol 55:261–268
13. Bergers G, Song S (2005) The role of pericytes in blood-vessel formation and maintenance. Neuro Oncol 7:452–464
14. Jacobs VL, Valdes PA, Hickey WF et al (2011) Current review of in vivo GBM rodent models: emphasis on the CNS-1 tumour model. ASN Neuro 3:e00063
15. Sampetrean O, Saga I, Nakanishi M et al (2011) Invasion precedes tumor mass formation in a malignant brain tumor model of genetically modified neural stem cells. Neoplasia 13:784–791
16. Bulnes S, Bengoetxea H, Ortuzar N et al (2012) Angiogenic signalling pathways altered in gliomas: selection mechanisms for more aggressive neoplastic subpopulations with invasive phenotype. J Signal Transduct 2012:597915
17. Morikawa S, Baluk P, Kaidoh T et al (2002) Abnormalities in pericytes on blood vessels and endothelial sprouts in tumors. Am J Pathol 160:985–1000
18. Hoffmann A, Bredno J, Wendland M et al (2011) High and low molecular weight fluorescein isothiocyanate (FITC)-dextrans to assess blood-brain barrier disruption: technical considerations. Transl Stroke Res 2:106–111
19. Matsui A, Yokoo H, Negishi Y et al (2012) CXCL17 expression by tumor cells recruits CD11b + Gr1 high F4/80-cells and promotes tumor progression. PLoS ONE 7:e44080
20. Sudou N, Garces-Vasconez A, Lopez-Latorre MA et al (2016) Transcription factors Mix1 and VegT, relocalization of vegt mRNA, and conserved endoderm and dorsal specification in frogs. Proc Natl Acad Sci USA 113:5628–5633
21. Charalambous C, Chen TC, Hofman FM (2006) Characteristics of tumor-associated endothelial cells derived from glioblastoma multiforme. Neurosurg Focus 20:E22
22. Hall AP (2006) Review of the pericyte during angiogenesis and its role in cancer and diabetic retinopathy. Toxicol Pathol 34:763–775
23. Nehls V, Denzer K, Drenckhahn D (1992) Pericyte involvement in capillary sprouting during angiogenesis in situ. Cell Tissue Res 270:469–474
24. Ozerdem U, Stallcup WB (2003) Early contribution of pericytes to angiogenic sprouting and tube formation. Angiogenesis 6:241–249
25. Baluk P, Morikawa S, Haskell A et al (2003) Abnormalities of basement membrane on blood vessels and endothelial sprouts in tumors. Am J Pathol 163:1801–1815
26. Morikawa S, Ezaki T (2011) Phenotypic changes and possible angiogenic roles of pericytes during wound healing in the mouse skin. Histol Histopathol 26:979–995
27. Mustafa DA, Burgers PC, Dekker LJ et al (2007) Identification of glioma neovascularization-related proteins by using MALDI-FTMS and nano-LC fractionation to microdissected tumor vessels. Mol Cell Proteomics 6:1147–1157
28. Wu ZB, Cai L, Lin SJ et al (2015) Heat shock protein 47 promotes glioma angiogenesis. Brain Pathol 26(1):31–42
29. Matsuoka Y, Kubota H, Adachi E et al (2004) Insufficient folding of type IV collagen and formation of abnormal basement membrane-like structure in embryoid bodies derived from Hsp47-null embryonic stem cells. Mol Biol Cell 15:4467–4475
30. Jeon H, Ono M, Kumagai C et al (1996) Pericytes from microvessel fragment produce type IV collagen and multiple laminin isoforms. Biosci Biotechnol Biochem 60:856–861
31. Inai T, Mancuso M, Hashizume H et al (2004) Inhibition of vascular endothelial growth factor (VEGF) signaling in cancer causes loss of endothelial fenestrations, regression of tumor vessels, and appearance of basement membrane ghosts. Am J Pathol 165:35–52
32. Mitsuhashi J, Morikawa S, Shimizu K et al (2013) Intravitreal injection of erythropoietin protects against retinal vascular regression at the early stage of diabetic retinopathy in streptozotocin-induced diabetic rats. Exp Eye Res 106:64–73
33. Holash J, Wiegand SJ, Yancopoulos GD (1999) New model of tumor angiogenesis: dynamic balance between vessel regression and growth mediated by angiopoietins and VEGF. Oncogene 18:5356–5362
34. Hillen F, Griffioen AW (2007) Tumour vascularization: sprouting angiogenesis and beyond. Cancer Metastasis Rev 26:489–502
35. Sa-Pereira I, Brites D, Brito MA (2012) Neurovascular unit: a focus on pericytes. Mol Neurobiol 45:327–347
36. Armulik A, Genove G, Betsholtz C (2011) Pericytes: developmental, physiological, and pathological perspectives, problems, and promises. Dev Cell 21:193–215
37. Betsholtz C (2004) Insight into the physiological functions of PDGF through genetic studies in mice. Cytokine Growth Factor Rev 15:215–228
38. Arentz G, Chataway T, Price TJ et al (2011) Desmin expression in colorectal cancer stroma correlates with advanced stage disease and marks angiogenic microvessels. Clin Proteomics 8:16
39. Gerhardt H, Betsholtz C (2003) Endothelial-pericyte interactions in angiogenesis. Cell Tissue Res 314:15–23